Interannual variability of summer monsoon rainfall onset date across India

Vincent Moron (*,**), Andrew W. Robertson (**)

(*) UFR des Sciences Géographiques et de l'Aménagement, Université d'Aix-Marseille, CEREGE, UMR 6635, and Institut Universitaire de France, France

(**) International Research Institute for Climate and Society (IRI), The Earth Institute, Columbia University, NY, USA

submitted to *Geophysical Research Letters*

13 February 2009

Abstract

Variability of Indian summer monsoon onset dates is investigated at 1-degree spatial resolution by applying an agronomic definition (i.e. the first significant rains without a potentially damaging dry spell thereafter) to gridded observed daily rainfall data (1951–2003). Median onset dates compare well with previous estimates. The inter-quartile range varies from less than two weeks over the monsoon zone and western Ghats, to about a month over the northwestern desert. Local onset date is shown to be poorly correlated with regional-scale definitions of monsoon onset, and this is attributed to low estimates of spatial coherence, found for local onset-date variability. There is a weak relationship between local onset date and the June–September seasonal rainfall total, while the latter is shown to be more spatially coherent—and thus more potential predictable—over the monsoon zone than local onset date.

1. Introduction

The onset of the monsoon rains is eagerly anticipated each summer over India. Its general northward, and westward, seasonal progression is well known from maps published by the Indian Meteorological Department (IMD), based on the long-term mean of the middle day of the pentad showing an abrupt increase of rainfall (see for example Fig. 1 of *Joseph et al.* [1994] or Fig. 1 of *Wang and LinHo* [2002]). Interannual variability of monsoon onset has generally been studied using univariate indices, the most famous being the date of the first rains over Kerala, located at the southernwestern tip of the India [*Ananthakrishnan and Soman*, 1988, 1989; *Raju et al.*, 2005], referred to hereafter as "MOK" (Monsoon onset over Kerala) following *Joseph et al.* [1994, 2006]. Both MOK and IMD reflect (uniquely and mostly, respectively) the first rains over Kerala. Later definitions have been based on regional-scale changes in circulation: *Fasullo and Webster* [2003] used the vertical integrated moisture transport (HOWI) averaged over the Arabian Sea while *Taniguchi and Koike* [2006] used the 850 hPa wind speed averaged over a similar area (WI); *Xavier et al.* [2007] offered a still larger-scale definition, based on previous analyses [i.e. *Krishnamurti et al.*, 1981; *Sonan and Krishna Kumar*, 1993; *Li and Yanai*, 1996], related to the reversal of the 600–200 hPa inter-hemipsheric temperature gradient, between a northern box (40–100E, 5–35N) and a southern one (40–100E, 15S–5N) (TTI). All these indices yield similar mean onset dates, between May 29 and June 5 [*Fasullo and Webster*, 2003; *Joseph et al.*, 2006; *Taniguchi and Koike*, 2006], but their relationships with the local onset of monsoon rains across India have not yet been studied in detail.

The goal of this paper is to analyze the variability of monsoon rainfall onset date at 1-degree spatial resolution, in terms of its spatial coherence, and relationships with the above regional indices, an index of ENSO, as well as the monsoon seasonal rainfall total. The spatial coherence of interannual anomalies of local rainfall is related to their potential seasonal predictability [i.e. *Moron et al.*, 2007], while robust relationship between local-scale onset and the above indices could potentially be used predictively on the weekly time scale, since the monsoon onset propagates northward and westward, Section 2 describes the 1-degree daily rainfall dataset and agronomic definition used to define local monsoon onset. The results of the statistical data analyses are given in Sect. 3, followed by concluding remarks in Sect. 4.

2. Data and definition of onset

We use the 1-degree gridded daily India rainfall data set for the 1951–2003 period, prepared by [*Rajeevan et al.*, 2006] from 1803 stations. Note that the resulting 357 gridboxes filter out rainfall variability at spatial scales below about 100 km.

Monsoon onset date is defined as the first wet day (> 1 mm) of the first 5-day wet sequence from April 1st that receives at least the climatological 5-day wet spell amount, without being followed by a 10-day dry spell (receiving less than 5 mm) in the following 30 days from the onset. This latter criterion is used to avoid “false starts” to the monsoon, related to pre-monsoon rainfall. There are 9.9% of gridbox/years with undefined onsets, mostly (> 50% of years) over the Thar desert of northwestern India in Gujarat and Rajasthan states (not shown). This is due to scattered nature of rainfall in this region, so that the false-start criterion is often not met. In fact, only 0.6% of gridbox/years do not have at least one 5-day wet sequence receiving at least the climatological amount of rain.

3. Results

a. Onset date distribution

Characteristics of the interannual distribution of onset dates over the 1951–2003 period are plotted for each gridbox in Fig. 1. The stippled region in Fig. 1a indicate gridboxes having a clear monsoonal regime with a maximum of rainfall in June-September, defined from a k-means cluster analysis of the low-pass filtered (< 1/120 cycle-per-day) mean annual cycle of daily rainfall amount. This region corresponds well with "monsoonal" India as defined by *Sikka and Gadgil* [1980], and is also referred to as the tropical convergence zone (TCZ).

Median onset dates (Fig. 1a) are similar to previous mean maps [*Joseph et al.*, 1994; *Wang and LinHo*, 2002], except for northeastern India, Kashmir and southeastern India. The first monsoonal rains appear in late April to mid May over Assam and the northeastern states, and near the southwestern tip of India. The arrival spreads rapidly from the regional-scale onset (late May to early June), firstly along the Western Ghats and western Bengal and Orissa, reaching most of monsoonal India by mid-July. The onset date appears somewhat earlier over Kerala and the northeastern states than in previous studies, while Kashmir and southeastern India are not influenced significantly by the summer monsoon.

Interannual variability of onset date is plotted in Fig. 1b in terms of the inter-quartile range (IQR). The IQR is less than 20 days over most of the TCZ and northeastern states, and increases toward drier parts of India; it is especially low over Orissa, and along the western Ghats. Much of the spatial modulation in IQR is reflected in the percentage of false starts (Fig. 1c), which is related to the risk of a dry spell following the first significant rains. The occurrence of a 10-day dry spell within a 30-day window from the first wet sequence is a rare event along the western coast, and over the eastern interior of the TCZ and northeastern states. The first significant wet sequence in these areas heralds the arrival of the monsoon, and interannual variation is rather limited—the local onset date here is a robust feature of the seasonal cycle. Over the dryer areas, the higher risk of a dry spell after the first significant rains increases the interannual variability of onset because it will delay the real onset in some years, leading to more erratic local onset date. The sensitivity to the 10-day dry spell criterion in the onset definition was tested by repeating the analyses using thresholds of 15 and 20 days (not shown). The results presented were found to be largely insensitive, with the exception of the percentage of false starts which necessarily increases. The dry spell criterion would need to be tuned in impact studies, for example according to the crop resistance to dryness.

Spatial coherence of onset date is plotted in Fig. 1d in terms of the conditional probability of onset occurring in all of the surrounding 8 gridboxes, given onset at the central point within a 10-day time window. This measures the "synchronization" of onset between neighboring 1-degree grid boxes. The highest spatial coherence is, not surprisingly, reached over the TCZ area, with lowest values near the boundaries between different seasonal rainfall regimes, such as between the TCZ and southeastern India.

b. Relationships with indices of onset

Next we analyze the relationships between gridded onset dates and the regional-scale onset indices. The MOK, IMD and HOWI indices were taken from Table 1 of *Joseph et al.* [2006], with WI obtained from *Taniguchi and Koike* [2006] and TTI from *Xavier et al.* [2007]. The cross-correlations between these indices range between 0.60 and 0.85 (average = 0.69) and the long-term mean of the standard deviation amongst the 5 indices equals 4.5 days. The deviations among the five indices exceed 10 days in some years, such as in 1969, 1974 or 1999 (not shown). In the following, we simply take the average of the five indices as the best empirical estimate of the regional-scale monsoon onset over the 1951–2003 time period (RSONS hereafter). Note that MOK is available only until 1990 while WI begins in 1979.

The correlations between RSONS and gridded agronomic onset are plotted in Fig. 2a. Statistical significance is assessed locally using a random-phase test [*Janicot et al.*, 1996] and tested globally using a Monte Carlo approach: 1000 random time series having the same FFT power spectrum as the regional-scale index but with random phases assigned to each Fourier component are correlated with the local onset and the proportion of locally significant correlations at the two-sided 95% level is computed. High correlations between RSONS and local onset date are found along the western coast, but surprisingly not exactly over Kerala. The correlations reach only moderate values over the eastern part of the TCZ where the onset is most robust according to Fig. 1, and where onset is near-contemporaneous in the mean with that defined by the indices (i.e. late May – early June). Despite the low proportion of locally significant values, the maps are significant at the 99% level due to the low spatial coherence (i.e. large number of degree of freedom) at interannual time scales. The correlations obtained with the individual monsoon indices (not shown) are similar to those in Fig. 2a; the largest correlations are attained with the largest scale index (i.e. TTI), while the smallest scale index (i.e. MOK) leads to the smallest values.

Interannual correlations between local onset date and the Niño 4 SST index (5S–5N, 160E–150W) are shown in Fig. 2b and exhibit a somewhat weaker though broadly similar pattern; the most consistent region of positive correlations is displaced slightly further north than in Fig. 2a. Similar patterns are obtained using the Niño3.4 index (5S–5N, 170W–120W), and using April or June SSTs (not shown). The weak relationship between local onset and the regional monsoon indices is consistent with the low spatial coherence of local onset date seen in Fig. 1. Additional measures of the low spatial coherence are given by the small fraction of the total variance (11.8%) explained by the leading EOF of local onset date (Fig. 3), and by the very small interannual variance (0.07) of the standardized anomaly index formed by the India-wide spatial average of standardized local onset dates. This value increases only slightly (0.10) when the TCZ region alone is considered. The loadings of EOF 1 (Fig 3a) reveal the spatial pattern of the weak common signal, with the largest loadings along the western coast and over the TCZ area, though extending more northwestward than do the significant correlations with the RSONS index. The principal component (PC) time series is plotted together with the RSONS index in Fig. 3b, with the whiskers on the RSONS giving the full range of its five component indices. The overall correlation is only 0.38, although there are several instances of common behavior, such as 1956, 1972, and 1998–2001. A robust regional-scale onset, as given by a small spread between the component regional indices is not necessarily related to a closer similarity between RSONS and PC 1 of local-scale onset. The correlations between the PC time series and the individual regional-scale indices are low (between 0.26 with MOK and 0.42 with WI).

c. Relationships with seasonal rainfall total

The low spatial coherence of local onset date suggests that year-to-year changes in the latter do not contribute much to the spatially-coherent common signal found in the interannual variability of seasonal rainfall total over the TCZ (e.g., *Gadgil* 2003, Fig. 4 there). Figure 4 shows the leading EOF of JJAS seasonal rainfall total, together with the correlations between the local onset date and local seasonal rainfall total. The leading PC explains 18% (19% for the TCZ area only) of the total variance of seasonal total across India. The pattern of the EOF resembles that of onset date, but with much larger loadings over the arid regions of northwestern India, and over the state of Jammu and Kashmir in the extreme north. The temporal correlation between the leading PCs of onset date and seasonal total is -0.34, suggesting a moderate regional-scale relationship between a late onset and a low seasonal total. At local scale, this relationship is most consistent over the eastern TCZ, consistent with EOF 1 of onset dates, as well as, perhaps more surprisingly, over Gujurat where loadings of the leading EOF of onset are small. The overall negative relationship is to be expected since onset occurs across most of India after June 1st (Fig. 1a). Considering JAS instead of JJAS reduces the number of significant (at the two-sided 95% level) local correlations from 36% to 15%, and the correlation between the respective leading PCs decreases from –0.34 to –0.18.

4. Concluding remarks

In this study, local gridded monsoon rainfall onset date is defined as the first significant rains without a potentially damaging dry spell thereafter. The latter criterion—no 10-day dry spell receiving less than 5 mm within the following 30 days—helps to discriminate false starts but may be too conservative for the driest part of India (the Thar Desert along the Pakistan border). Nevertheless, the median onset date appears to be consistent with previous precise estimates published by IMD (see *Joseph et al.* [1994] and *Wang and LinHo* [2002]). The local-scale onset is especially robust (i.e. small risk of "false" starts, weak interannual variability, strongest synchronization of onset) over the Western Ghats and the eastern part of the TCZ area of *Gadgil* [2003].

The spatial coherence at interannual time scale is at best moderate, suggesting a low level of potential predictability related to large-scale forcings (e.g. sea surface temperatures over Pacific and Indian oceans, snow cover over Tibetan plateau, etc.). Similarly, the correlations between regional-scale and local onsets are not very high, even when the latter are spatially averaged. This suggests that even if regional-scale onset is able to trigger local-scale monsoon rainfall, the latter are a product of meso- to synoptic scale phenomena whose size, intensity and/or tracks are poorly reproducible from one year to another. More work is nevertheless needed regarding the relationship between intraseasonal oscillations and the spatial scales of onset. The weak spatial coherence of local monsoon rainfall onset dates over India is not a ubiquitous result across the tropics. Over Indonesia and the Philippines, a significant component of seasonal potential predictability at local scale has been shown to be associated with monsoon onset date [*Moron et al.*, 2009a,b]. In the case of India, advances and delays in local onset do contribute to anomalies in monsoon seasonal rainfall total over the TCZ region, although removing June decreases the strength of the relationship. Thus, as in the case of Indonesia [*Moron et al.*, 2009a], while onset anomalies influence the length of the monsoon season to some extent, they do not foreshadow anomalies within the monsoon season itself.

Acknowledgements: We are grateful to the National Climate Centre of the India Meteorological Department for making the daily rainfall data available. This research was supported by grants from the National Oceanic and Atmospheric Administration (NOAA), NA050AR4311004, and the US Department of Energy's Climate Change Prediction Program, DE-FG02-02ER63413.

References

Ananthakrishnan R., and M.K. Soman (1988) The onset of the south-west monsoon over Kerala: 1901-1980, *J. Climatol.*, *8*, 283-296.

Ananthakrishnan R., and M.K. Soman (1989) Onset dates of the south-west monsoon over Kerala for the period 1870-1900, *Int. J. Climatol.*, *9*, 321-322.

Fasullo J., and P.J. Webster (2003) A hydrological definition of Indian Monsoon onset and withdrawal, *J. Clim.*, *16*, 3200-3211.

Gadgil S. (2003) The Indian monsoon and its variability, *Ann. Rev. Planet Sci.*, *31*, 429-467.

Janicot S., V. Moron, and B. Fontaine (1996) ENSO and Sahel droughts, *Geophys. Res. Lett.*, *23*, 515-518.

Joseph P.V., J.K Eischeid, and R.J. Pyle (1994) Interannual variability of the onset of the Indian summer monsoon and its association with atmospheric features, El Niño and sea surface temperatures anomalies, *J. Clim.*, *7*, 81-105.

Joseph P.V., K.P. Sooraj, and C.K Rajan (2006) The summer monsoon onset process over South Asia and an objective method for the date of monsoon onset over Kerala, *Int. J. Climatology*, *26*, 1871-1893. Doi: 10.1002/joc.1340.

Krishnamuri T.N., P. Ardanuy, Y. Ramanathan and R. Pasch (1981) On the onset vortex of the summer monsoon, *Mon. Wea. Rev.*, *109*, 344-363.

Li C., and M. Yanai (1996) The onset and interannual variability of the Asian summer monsoon in relation to Land-Sea thermal contrast. *J. Clim.*, *9*, 358-375.

Moron V., A.W. Robertson, M.N. Ward, and P. Camberlin (2007) Spatial coherence of tropical rainfall at the regional scale. *J. Clim.*, *20*, 5244-5263.

Moron V., A.W. Robertson, and R. Boer (2009a) Spatial coherence and seasonal predictability of monsoon onset over Indonesia, *J. Clim.*, *22*, 841-851.

Moron V., A. Lucero, F. Hilario, B. Lyon, A.W. Robertson, and D. DeWitt (2009b) Spatio-temporal variability and predictability of summer monsoon onset over the Philippines. *Clim. Dyn.*, in press.

Rajeevan M., J. Bhate, J. Kale, and B. Lal (2006) Development of a High resolution daily gridded rainfall data for the Indian region. Met. Monograph Climatology n° 22/2005. India Meteorological Department.

Raju P.V.S., U.C. Mohanty, and B. Bhatla (2005) Onset characteristics of the southwest monsoon over India, *Int. J. Climatol.*, *25*, 167-182.

Sikka D.R., and S. Gadgil (1980) On the maximum cloud zone and the ITCZ over India longitude during the Southwest monsoon. *Mon. Wea. Rev.*, *108*, 1840-1853.

Soman M.K., and M. Krishna Kumar (1993) Space-time evolution of Meteorological Features - associated with the onset of Indian summer monsoon, *Mon. Wea. Rev.*, *121*, 1177-1194.

Taniguchi K., and T. Koike (2006) Comparison of definitions of Indian summer monsoon onset: better representation of rapid transitions of atmospheric conditions, *Geophys. Res. Letters*, *33*, L02709, doi:10.1029/2005GL0245226.

Wang B., and LinHo (2002) Rainy season of the Asian-Pacific summer monsoon. *J. Clim.*, *15*, 386-398.

Xavier P.K., C. Marzin, and B.N. Goswami (2007) An objective definition of the Indian summer monsoon season and a new perspective of the ENSO-monsoon relationship. *Quart. J. Meteo. Soc.*, *133*, 749-764, doi:10.1002/qj.45.

Figure Captions

Figure 1: (a) Median and, (b) inter-quartile range (IQR) of local onset dates. (c) Percentage of false starts defined as a mismatch between the first 5-day wet spell receiving at least the mean amount of a 5-day wet sequence and the local onset date defined in the text. An undefined onset is also considered as a false start. (d) Conditional probability of onset within the 8 surrounding gridboxes, given the onset occurs at the central gridbox. A 10-day window is used centered on the local-scale onset. at the base gridbox. The black dots on panel (a) indicate the Tropical Convergence Zone (TCZ); see text.

Figure 2 : (a) Correlations between local onset and the index of regional-scale onset (RSONS) defined in the text. (b) Correlations between local onset and the Niño4 SST index in May. Crosses indicate statistically significant correlations at the two-sided 95% level (see text). The value in parenthesis gives the fraction of significant gridboxes.

Figure 3: (a) Leading EOF of local onset, plotted as correlation coefficients with the PC time series. Crosses indicate statistically significant correlations at the two-sided 95% level (see text). The value in parenthesis gives the explained variance and fraction of significant gridboxes. (b) Time series of leading PC (red) and regional-scale onset index (RSONS). Vertical bars denote the spread of the five regional-scale indices that make up RSONS. All time series are standardized to zero mean and unit variance.

Figure 4 : (a) Leading EOF of JJAS rainfall total, plotted as correlation coefficients with the PC time series. (b) Correlations between local onset date and local JJAS rainfall total. Crosses indicate

statistically significant correlations at the two-sided 95% level (see text). The value in parenthesis gives the fraction of significant gridboxes, together with the explained variance in (a).

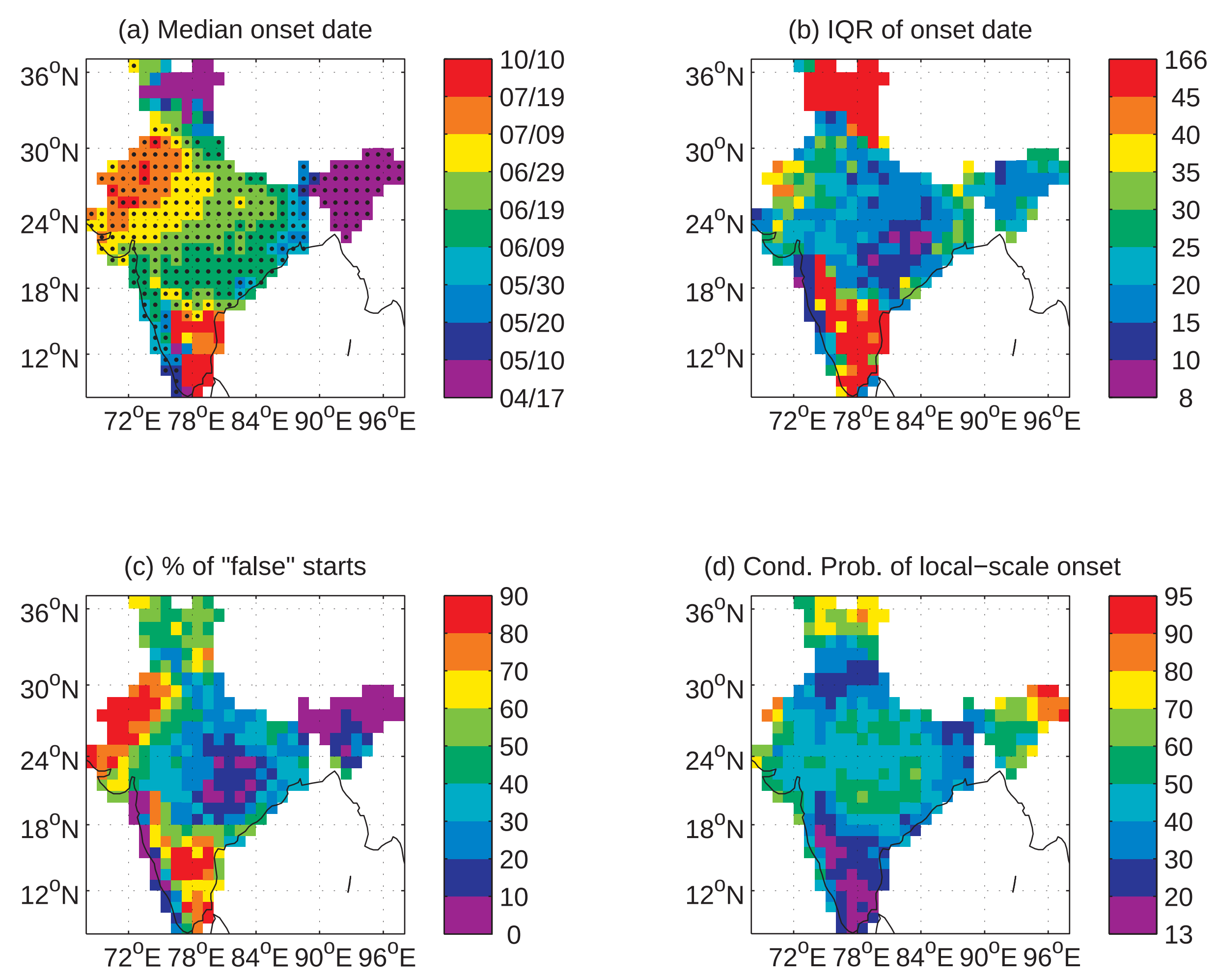
(a) Median onset date
(b) IQR of onset date
(c) % of "false" starts
(d) Cond. Prob. of local−scale onset
36°N
30°N
24°N
18°N
12°N
72°E 78°E 84°E 90°E 96°E
10/10
07/19
07/09
06/29
06/19
06/09
05/30
05/20
05/10
04/17
166
45
40
35
30
25
20
15
10
8
90
80
70
60
50
40
30
20
10
0
95
90
80
70
60
50
40
30
20
13

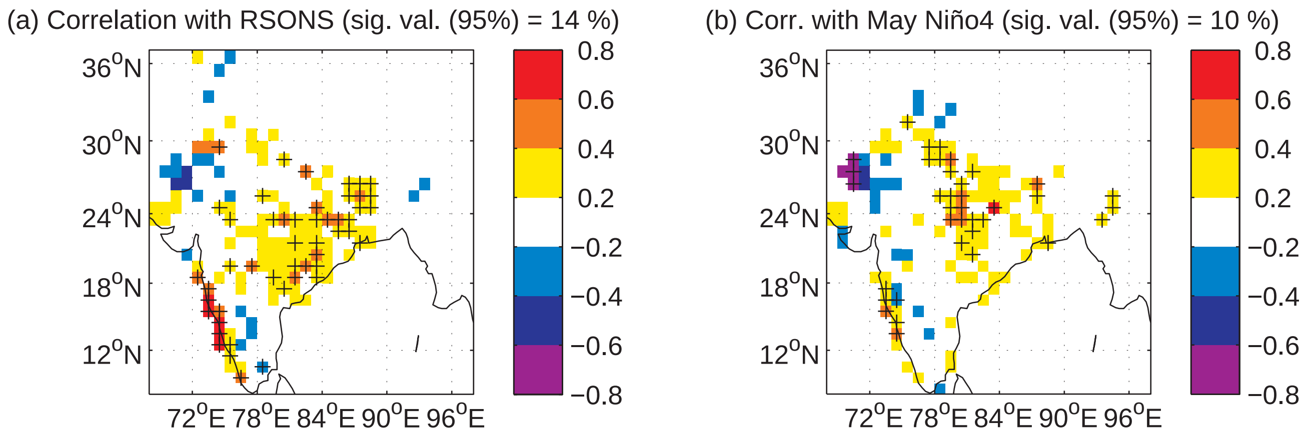
(a) Correlation with RSONS (sig. val. (95%) = 14 %)
(b) Corr. with May Niño4 (sig. val. (95%) = 10 %)
36°N
30°N
24°N
18°N
12°N
72°E 78°E 84°E 90°E 96°E
0.8
0.6
0.4
0.2
−0.2
−0.4
−0.6
−0.8

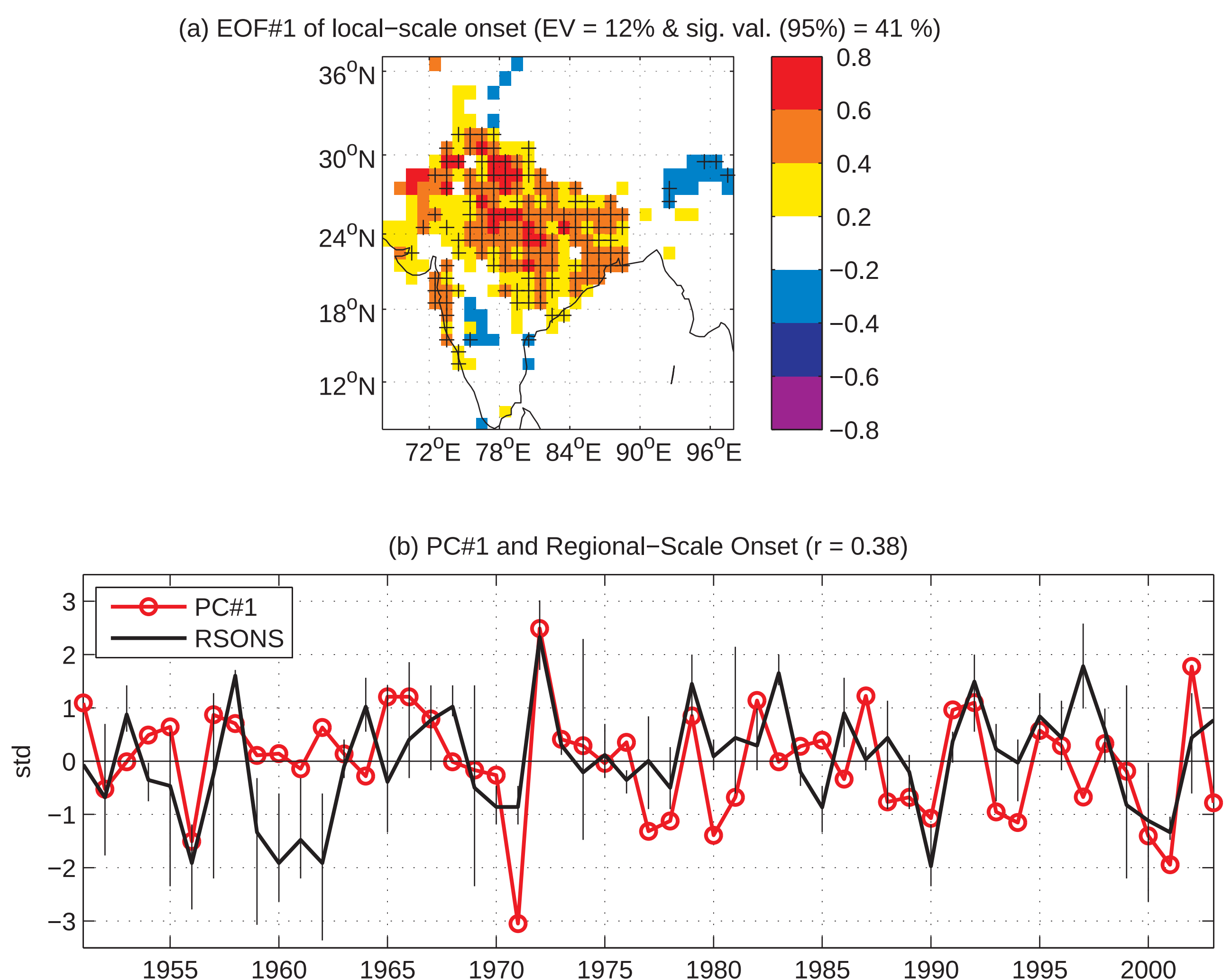
(a) EOF#1 of local−scale onset (EV = 12% & sig. val. (95%) = 41 %)
36°N
30°N
24°N
18°N
12°N
72°E
78°E
84°E
90°E
96°E
0.8
0.6
0.4
0.2
−0.2
−0.4
−0.6
−0.8
(b) PC#1 and Regional−Scale Onset (r = 0.38)
PC#1
RSONS
std
3
2
1
0
−1
−2
−3
1955
1960
1965
1970
1975
1980
1985
1990
1995
2000

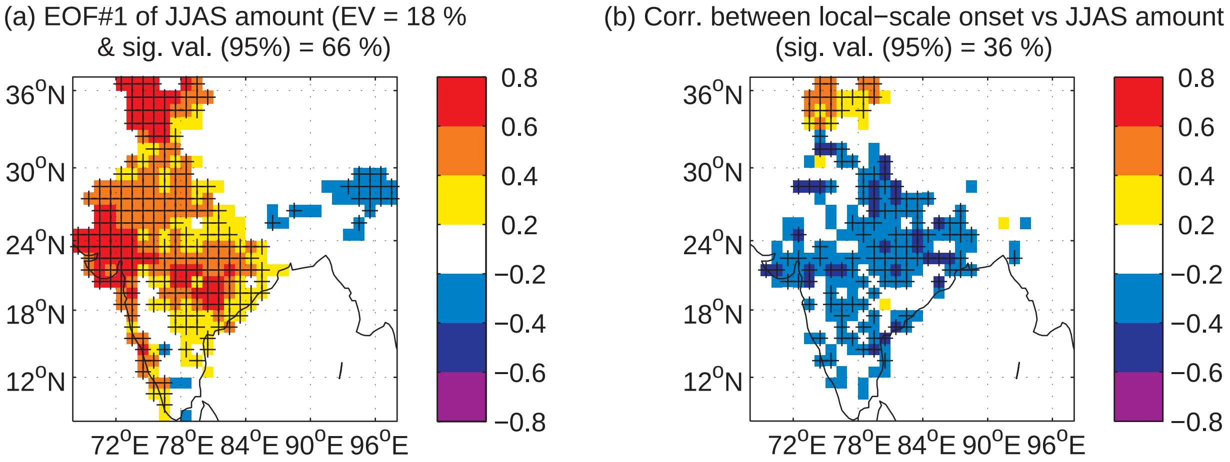

(a) EOF#1 of JJAS amount (EV = 18 %
& sig. val. (95%) = 66 %)
(b) Corr. between local−scale onset vs JJAS amount
(sig. val. (95%) = 36 %)
36°N
30°N
24°N
18°N
12°N
72°E 78°E 84°E 90°E 96°E
0.8
0.6
0.4
0.2
−0.2
−0.4
−0.6
−0.8